

# LABYRINTH SEALS DYNAMIC COEFFICIENTS AND CRITICAL SPEED RESEARCH BASED ON CHILDS' MODEL

**Ma Wensheng, Huang Hai, Feng Guoquan**  
**AVIC Shenyang Aeroengine Research Institute, Shenyang, China**

*Keywords: labyrinth seals, dynamics coefficients, critical speed, Childs' model*

## Abstract

*Mathematical method are used to calculate the dynamic coefficients and Critical of labyrinth seals. It is important to know the accurate dynamic coefficients of labyrinth seals for predicting the instability of the rotor-seal system. Labyrinth seal dynamic coefficients at different radial clearances, pre-swirl ratios, rotor speeds, seal lengths and diameters are presented in this paper. Critical speed at different seal length and diameters are also studied in this paper.*

## 1 Title of Section (e.g. General Introduction)

Labyrinth seals are non-contacting annular seals, and are widely used in steam turbines, gas turbines and gas compressors. The labyrinth seal has many advantages, such as simplicity, reliability, and tolerance for high temperature and high pressure. The labyrinth seal has improved over the years. There were several major stages in the development of methods to study the forces and dynamic coefficients of the seal: experiments, bulk flow, and finite volume methods. Each stage led to a new understanding about the performance and dynamic characteristics of labyrinth seals.

Originally, most of the work focused upon experimental data and simplified rotordynamic systems. Alford [1] studied a labyrinth seal with varying inlet and outlet areas. He concluded that when the inlet area exceeds the outlet area, an excitation force is produced that causes rotor in the direction of the rotation. Conversely, Alford concluded that no excitation force would be produced when the outlet area exceeds the inlet area. These conclusions have unfortunately

resulted in undesirable results in high pressure centrifugal compressors labyrinth seals. More experimental work was carried out by Bencker and Wachter [2], and they were able to calculate spring coefficients for the seals. A bulk flow design code for labyrinth seals was developed by Kirk [3] and the results were used to evaluate rotor system stability that were favorably compared to the resulting stability of compressors on test and in the field. Rajakumar and Sisto [4] more recently performed experiments to determine the circumferential pressure distributions and forces within a labyrinth seal.

Starting in the mid 1980s, more robust methods were brought into use to study the dynamic coefficients of a labyrinth seal. There were two main methods used: bulk flow and finite volume. Wyssmann et al. [5] used a two control volume approach to model the flow through a labyrinth seal. The two control volume approach is a simplified approach to a finite volume method. For that reason, the modeled flow through the seal was oversimplified and could only be used for general comparisons and trends. Rhode and Sobolik [6] used a finite difference approximation to predict the leakage flow through a labyrinth seal. R. Nordmann [7] got rotordynamic coefficients of turbine labyrinth seals by the comparison CFD models and experiments.

## 2 Labyrinth Seal Coefficients

This research focuses on the stage centrifugal compressor impeller eye labyrinth seal coefficients. The impeller eye labyrinth seal is used to reduce leakage and facilitate a

pressure drop from the high pressure discharge into the region of lower pressure inlet flow. This is accomplished by creating a flow path for the working fluid that converts the pressure head into kinetic energy. The kinetic energy is then dissipated. The straight labyrinth can be divided into two categories: tooth-on-stator and tooth-on-rotor. A tooth on rotor labyrinth seal is shown in Fig 1. Figure 2 shows a tooth on stator labyrinth seal with selected nomenclature. Table 1 and Table 2 show the dimensions and conditions used for the calculations to be discussed in this paper. This calculation assumes the fluid to be an ideal gas and the entire flow to be turbulent. The k- $\epsilon$  model is used for turbulence.

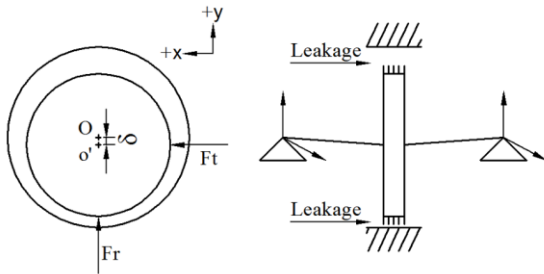


Figure 1 Jeffcott rotor-seal system

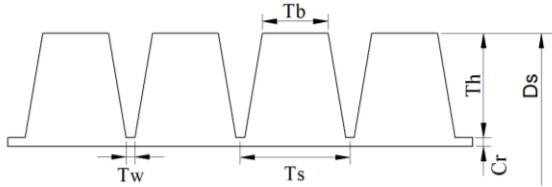


Figure 2 Straight labyrinth seal dimensions

Table. 1 Labyrinth Seal Geometric Dimensions

Dimension	Value
Diameter, Ds	150mm
Radial Clearance, Cr	0.3mm
Pitch, Ts	4mm
Height, Th	3.5mm
Tip width, Tw	0.3mm
Number of Teeth	5

Table. 2 Seal Operating Conditions

Dimension	Value
Speed	10331RPM
Inlet Pressure	10.68MPa
Discharge Pressure	8.28MPa
Inlet Temperature	52.2 °C
Discharge Temperature	22.2 °C
Gas	Air
Turbulence model	k- $\epsilon$

### 3 Labyrinth seals dynamics model

Childs formulated a bulk flow model using Hirs' lubrication equation, which the linearized forces acting on the rotor generated in a seal are:

$$-\begin{bmatrix} F_x \\ F_y \end{bmatrix} = \begin{bmatrix} k_{xx} & k_{xy} \\ k_{xy} & k_{xx} \end{bmatrix} \begin{bmatrix} x \\ y \end{bmatrix} + \begin{bmatrix} c_{xx} & c_{xy} \\ c_{xy} & c_{xx} \end{bmatrix} \begin{bmatrix} \dot{x} \\ \dot{y} \end{bmatrix} + \begin{bmatrix} m_f \\ m_f \end{bmatrix} \begin{bmatrix} \ddot{x} \\ \ddot{y} \end{bmatrix} \quad (1)$$

The restoring forces are proportional to displacement, velocity and acceleration. A fundamental relationship between the total axial pressure drop and the mean axial gas velocity is:

$$\Delta P = \frac{1}{2}(1 + \xi + 2\sigma)\rho V^2 \quad (2)$$

Where

$$\sigma = \lambda \frac{L}{Cr} \quad (3)$$

and  $\frac{1}{2}(1 + \xi)\rho V^2$  defines the inlet pressure

drop. It shows that the inlet pressure drop is greater in the region where the clearance is larger due to high velocity than the region where the clearance is small. Childs formulated the seal dynamic coefficients based on Hirs' lubrication equation, which included in the momentum equations and the inlet swirl is also included. The circumferential velocity of the gas entering the seal is commonly expressed as a fraction of shaft surface speed ( $R\Omega$ ):

$$u_c = \alpha R\Omega \quad (4)$$

The coefficients are summarized in the following:

$$k_{xx} = \left( \frac{\pi R \Delta P}{\lambda} \right) \frac{2\sigma^2}{1 + \xi + 2\sigma} \quad (5)$$

$$k_{xy} = \left( \frac{\pi R \Delta P}{\lambda} \right) \frac{\sigma^2 \Omega T}{1 + \xi + 2\sigma} \left[ \frac{E}{\sigma} + \frac{B}{2} \left( \frac{1}{6} + E \right) + \frac{2v_0}{a} \left[ \frac{EB + \left( \frac{1}{\sigma} - \frac{B}{a} \right)}{1 - e^{-a} \left( E + \frac{1}{2} + \frac{1}{a} \right)} - 1 \right] \right] \quad (6)$$

$$c_{xx} = \left( \frac{\pi R \Delta P}{\lambda} \right) \frac{2\sigma^2 T}{1 + \xi + 2\sigma} \left[ \frac{E}{\sigma} + \frac{B}{2} \left( \frac{1}{6} + E \right) \right] \quad (7)$$

$$c_{xy} = \left( \frac{\pi R \Delta P}{\lambda} \right) \frac{2\sigma^2 \Omega T}{1 + \xi + 2\sigma} \left[ \frac{1}{2} \left( \frac{1}{6} + E \right) + \frac{v_0}{a} \left[ \frac{1 - e^{-a}}{E + \frac{1}{2} + \frac{1}{a}} - \left( \frac{1}{2} + \frac{e^{-a}}{a} \right) \right] \right] \quad (8)$$

$$m_f = \left( \frac{\pi R \Delta P}{\lambda} \right) \frac{\sigma \left( \frac{1}{6} + E \right)}{1 + \xi + 2\sigma} T^2 \quad (9)$$

where

$$\lambda = 0.066R_a^{0.25} \left(1 + \frac{1}{4b^2}\right)^{0.375} \quad (10)$$

$$R_a = \frac{\rho V C r}{\mu} \quad (11)$$

$$R_c = \frac{\rho R \Omega C r}{\mu} \quad (12)$$

$$b = \frac{R_a}{R_c} = \frac{V}{R \Omega} \quad (13)$$

$$a = \sigma(1 + 0.75\beta) \quad (14)$$

$$\beta = \frac{1}{1 + 4b^2} \quad (15)$$

$$B = 1 + 3b^2\beta \quad (16)$$

$$E = \frac{1 + \xi}{2(1 + \xi + B\sigma)} \quad (17)$$

$$T = \frac{L}{V} \quad (18)$$

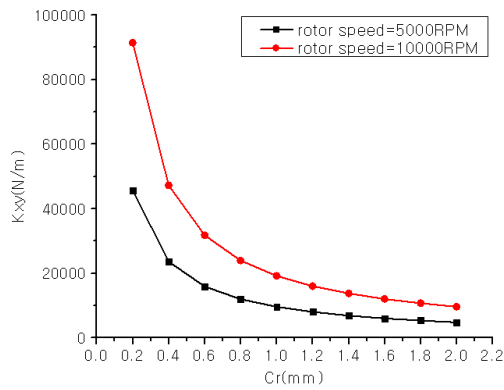
#### 4 Labyrinth Seal Dynamics Coefficients Study

Results for the labyrinth seal model of Fig 2 using Childs' experimental conditions [15] are shown in Fig 8. The labyrinth seal geometric conditions are follows: Seal length is 15.2 mm, seal diameter is 150 mm and radial clearance is 0.3mm. The results are presented as dynamic coefficients versus rotor speed, pre-swirl, seal length and labyrinth seal clearance. The Childs' experimental conditions were air temperature 300K, air density 1.225kg/m<sup>3</sup>, and pressure 8.28 × 10<sup>6</sup> Pa. Cross-coupled stiffness is a major reason of instability in bearings, hence the labyrinth seal system is more likely to be unstable when the cross-coupled stiffness is greater. It is also known that direct damping can improve system stability, hence cross-coupled stiffness and direct damping are the main research in this paper.

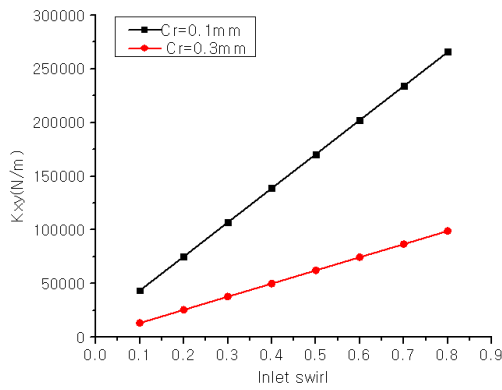
Figure 3(a) shows the relation of labyrinth seal radial clearance and cross-coupled stiffness for different rotor speeds. Rotor speed is shown for 5000 rpm and 10000 rpm. Figure 3(a) shows that cross-coupled stiffness will decrease as the

labyrinth seal clearance is increasing. The cross-coupled stiffness decreased sharply when the labyrinth radial clearance increased from 0.2mm to 2mm, but they changed little when the labyrinth seal clearance is more than 0.2mm. The seal has less destabilizing cross-coupled stiffness when labyrinth seal radial clearance is more than 0.2mm. Figure 3(b) gives the result for labyrinth seal cross-coupled stiffness for two different labyrinth seal clearances plotted versus pre-swirl ratio. The two labyrinth seal clearances used were 0.1 mm and 0.3 mm. This result clearly shows that the cross-stiffness will increase with a higher pre-swirl ratio. Labyrinth radial clearance is made as small as possible to control leakage in a real machine, so it is a better practice to make the labyrinth system more stable by reducing the pre-swirl ratio with mechanical or aerodynamic swirl brakes.

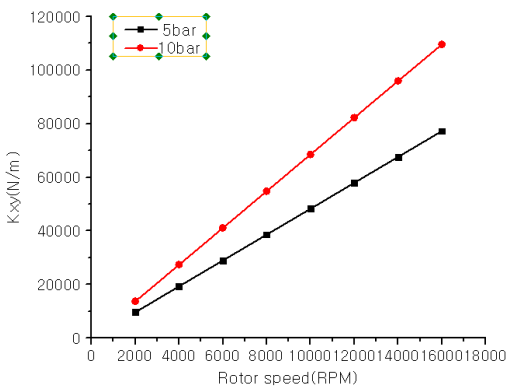
Figure 3(c) show cross-coupled stiffness for three different pressure drops plotted versus rotor speed, the three pressures being 5 × 10<sup>5</sup>Pa and 10 × 10<sup>5</sup>Pa. It can be seen that cross-coupled stiffness will increase with rotor speed and also as the pressure drop increases. Hence a system will be less stable as rotor speed and pressure drop increase. However the dynamics of a machine will be more stable for a stiffer shaft and higher critical speed, so the important parameter to reduce when possible is the pressure drop. Figure 3(d) shows the direct damping for different labyrinth seal diameters plotted versus seal length. Labyrinth seal length varies from 6 mm to 20 mm, and the labyrinth seal diameters are 100 mm and 150 mm. Figure 3(d) shows that the direct damping will increase as labyrinth seal length increases and also as the labyrinth seal diameter increases. From a practical standpoint, a reduction in diameter is the important method to reduce the destabilizing forces in a seal.



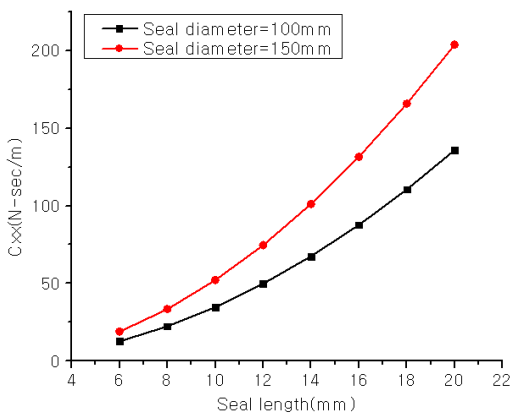
(a) Cross-coupled stiffness versus seal clearance



(b) Cross-coupled stiffness versus ratio of pre-swirl ratio



(c) Cross-coupled stiffness versus rotor speed

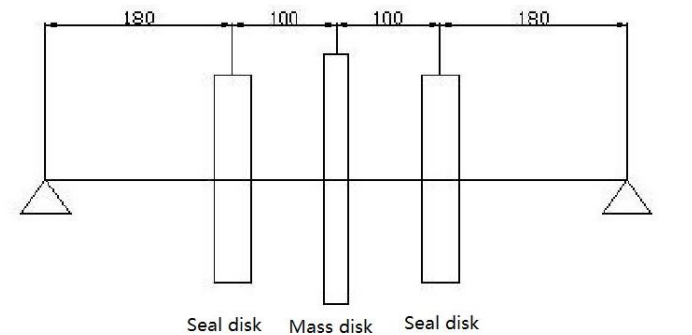


(d) Direct damping versus seal length

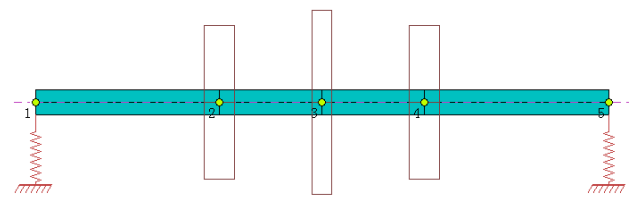
Figure 3 Labyrinth seal dynamics coefficients effect factors

### 5 Critical Speed Study

Fig.4 (a) is rotor-bearing-seal system model which include shaft, bearing, seal disk and mass disk. The shaft length is 560 mm, the shaft disk spacing is 100mm. The seal disk is 10 kg and mass disk is 15 kg in this model. The geometric conditions are shown in the Tab.1 and operating conditions are shown in the Tab.2. Rotor-bearing-seal DyRoBes model is shown in Fig.8 (b). It can calculate rotor-bearing-seal critical speed mode shape as shown in Fig.5. First-order critical speed mode shape is shown in Fig.5 (a) and second-order critical speed mode shape is shown in Fig.5 (b).



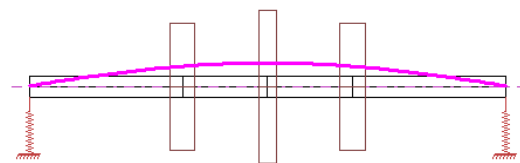
(a) Rotor-bearing-seal system dimensions



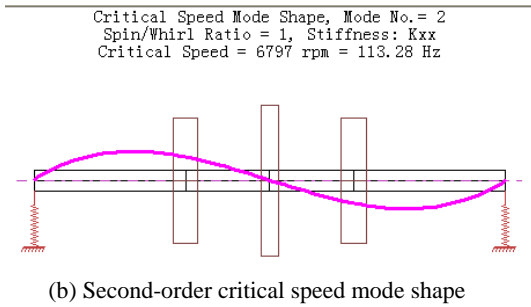
(b) Rotor-bearing-seal system DyRoBes model

Figure 5 Rotor-bearing-seal system model

Critical Speed Mode Shape, Mode No.= 1  
Spin/Whirl Ratio = 1, Stiffness: Kxx  
Critical Speed = 1504 rpm = 25.06 Hz



(a) First-order critical speed mode shape



(Seal diameter=150mm)

Figure 5 Rotor-bearing-seal system critical speed mode shape

Fig.6 is rotor-bearing-seal system critical speed effect study in different seal length when the seal diameter is 100mm. Fig.7 is rotor-bearing-seal system critical speed effect study in different seal length when the seal diameter is 150mm. Fig.6 and Fig.7 shows the seal length effect to first-order critical speed. Seal length is shown for 6 mm and 20 mm. The results show that first-order critical speed will increase as the seal length is increasing.

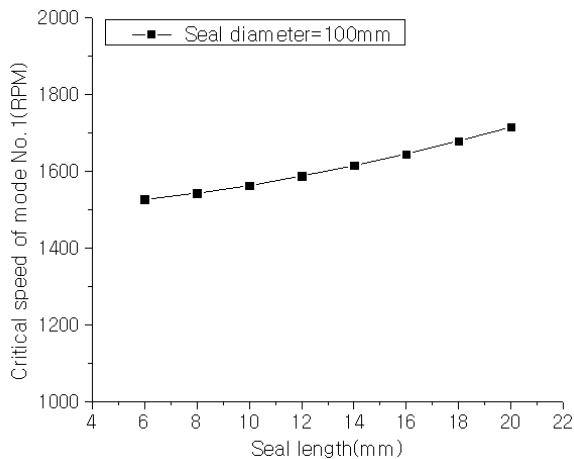


Figure 6 Critical speed of different seal length  
(Seal diameter=100mm)

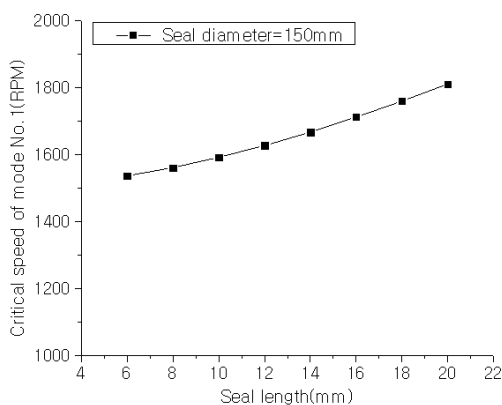


Figure 7 Critical speed of different seal length

## 6 Conclusions

The paper presents the impact of rotor labyrinth seal dynamic coefficients and critical speed by mathematical method. The seal clearance, pre-swirl ratio, seal length, seal diameter were varied to determine the effect on compressible flow pattern for the labyrinth seal dynamics coefficients and critical speed.

Labyrinth seal clearance could be increased to reduce the instability caused by cross-coupled stiffness. A system will be less stable when rotor speed, pressure, seal length and seal diameter are increasing. The labyrinth seal system can have better stability when the labyrinth seal clearance is increasing.

## References

- [1] Alford, J. S (1965). Protecting turbomachinery from self-excited rotor whirl. *Journal of Engineering for Power*, v. 87, 333-334.
- [2] Benckert, H. Wachter, J. (1980). Flow induced spring coefficients of labyrinth seals for application in rotor dynamics. *NASA CP 2133*, 189-212.
- [3] Kirk, R.G (1988). Evaluation of aerodynamic instability mechanisms for centrifugal compressors – part II: advanced analysis. *Journal of Vibration, Acoustics, Stress, and Reliability in Design*, v. 110, 207-212.
- [4] Rajakumar, C. Sisto, F. (1990). Experimental investigations of rotor whirl excitation forces induced by labyrinth seal flow. *Journal of Engineering for Gas Turbines and Power*, v. 106, 263-272.
- [5] Wyssmann, H.R., Pham T.C., Jenny R.J. (1984). Prediction of stiffness and damping coefficients for centrifugal compressor labyrinth seals. *Journal of Engineering for Gas turbines and Power*, v.106, 920-926.
- [6] Rhode D.L. Sobolik S.R. (1986). Simulation of subsonic flow through a generic labyrinth seal. *Journal of Engineering for Gas Turbines and Power*, v. 108, 674-680.
- [7] J. Schettel and R. Nordmann. (2004). Rotordynamics of turbine labyrinth seals-a comparison of CFD models to experiments. *IMECHE 8th International Conference on Vibrations in Rotating Machinery*.

## Contact Author Email Address

Email: mawensheng1980@gmail.com

### **Copyright Statement**

The authors confirm that they hold copyright on all of the original material included in this paper. The authors also confirm that they have obtained permission, from the copyright holder of any third party material included in this paper, to publish it as part of their paper. The authors confirm that they give permission, or have obtained permission from the copyright holder of this paper, for the publication and distribution of this paper as part of the ICAS proceedings or as individual off-prints from the proceedings.